In situ photoluminescence/Raman study of reversible photo-induced structural transformation of nc-Si

2014 Mater. Res. Express 1 045905

(http://iopscience.iop.org/2053-1591/1/4/045905)

Materials Research
Express

In situ photoluminescence/Raman study of reversible photo-induced structural transformation of nc-Si

V O Yukhymchuk[1], V M Dzhagan[1,2], M Ya Valakh[1], V P Klad'ko[1], O J Gudymenko[1], V S Yefanov[3] and D R T Zahn[2]

[1] V. Lashkaryov Institute of Semiconductors Physics, National Acad. Sci. of Ukraine, Kyiv, Ukraine
[2] Semiconductor Physics, Technische Universität Chemnitz, Chemnitz, Germany
[3] OOO 'NanoMedTekh', Kyiv, Ukraine
E-mail: volodymyr.dzhagan@physik.tu-chemnitz.de

Received 14 August 2014, revised 5 October 2014
Accepted for publication 12 October 2014
Published 5 November 2014

Materials Research Express **1** (2014) 045905

doi:10.1088/2053-1591/1/4/045905

Abstract

A cubic-to-hexagonal phase transition in Si nanocrystals (NCs) is observed *in situ* by recording their Raman and photoluminescence (PL) spectra simultaneously. The formation of the hexagonal structure is concluded from the appearance of characteristic Raman peaks and intense PL with spectral positions reported previously for hexagonal Si. The phase transition occurs due to heating of the NCs by the laser beam, but it is supposed to be a photo-induced effect, as it does not occur as a consequence of solely thermal heating. Both the structural transition and concomitant switching of the bright PL emission are reversible and are supposed to be of interest from the viewpoint of application.

Keywords: silicon, nanocrystals, hexagonal, transition, Raman, photoluminescence

1. Introduction

Silicon nanocrystals (NCs) have shown great potential in a range of applications [1–4]. Like other semiconductor materials, when Si crystallites are made smaller than the exciton Bohr radius, their electronic and light emission properties can be tuned via size-dependent quantum confinement and further modified by surface chemistry [4, 5]. The photoluminescence (PL) emission of Si NCs has been the matter of a long-standing discussion [1, 4, 6–8]. Usually Si crystallizes in the cubic diamond structure [2, 3, 6]. However, several other Si polytypes are known, which are stable in bulk only at high pressures [9], but can be stabilized at ambient pressure in Si nanowires [10]. Among these polytypes, hexagonal Si (h-Si) is the most often reported one and promising for novel optoelectronic applications due to its linear and nonlinear

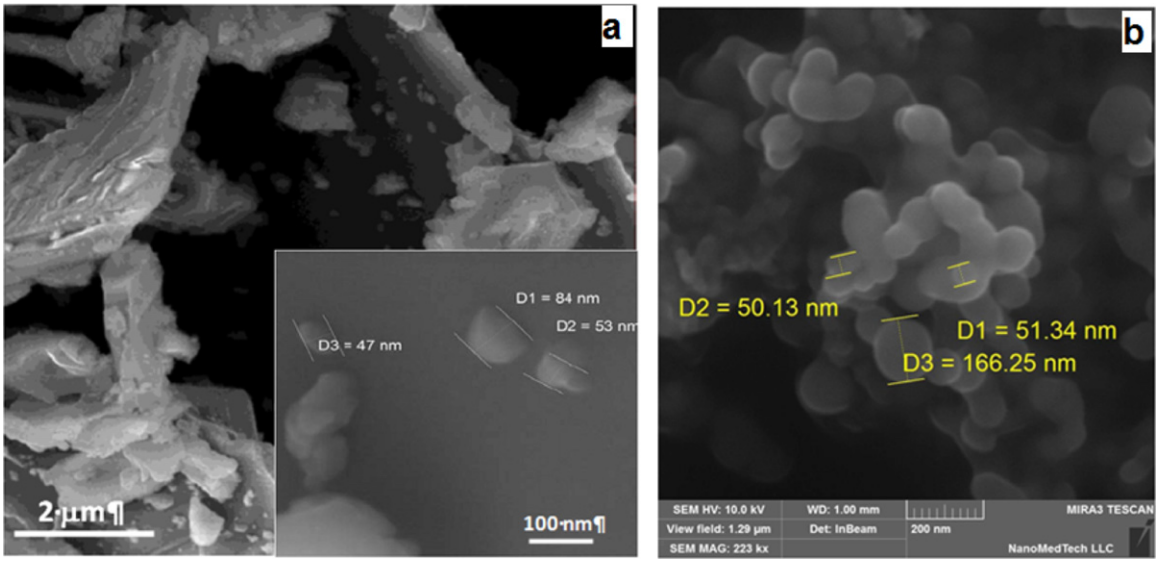

Figure 1. SEM images of sample 1(a) and sample 2(b).

optical properties [11–17]. The formation of the h-Si phase was observed in stressed amorphous Si (a-Si) [18], in Si nanowires [19–24], or in SiC matrices [16]. In most cases the formation of h-Si is induced by stress. The hexagonal structure of Si can be distinguished from the cubic one by Raman spectroscopy, because its characteristic optical phonon frequencies are shifted downwards from the phonon mode of cubic Si, peaked at 520 cm^{-1} [16, 25]. However, in some studies, the Raman features appearing well below 520 cm^{-1} and observed at intense illumination of Si nanostructures were explained as surface modes [27–30] or 'forbidden' optical phonon modes of the cubic phase [23]. Thus, the nature of these Raman features still needs to be clarified.

Here we report the results of a Raman/PL study of Si NCs, where we observe splitting of the Raman peak at certain power of the laser excitation (P_{exc}) accompanied by the appearance of an intense red PL. Based on the spectral positions of the appearing Raman and PL bands, we conclude that a structural transition from cubic to h-Si occurs. This transition can be monitored *in situ* by Raman and PL spectra simultaneously and reversibly controlled by adjusting P_{exc}.

2. Experimental

Two kinds of Si samples were studied. Sample 1 was obtained by grinding of silicon plates in a ball mill resulting in a rather quasi-continuous distribution of crystallite sizes in the nano- and micrometer range, as can be seen from the scanning electron microscopy (SEM) image (figure 1). Sample 2 was commercially available 'NanoAmor' Si NCs with an average size of 100 nm.

The SEM images were acquired in this work using Mira 3 Tescan microscope. The Raman/PL spectra were excited with $\lambda_{exc} = 488.0$ or 514.5 nm of an Ar^+ laser or 632.8 nm of a He–Ne laser and recorded using a LabRam HR800 micro-Raman system (100× objective). The power of the laser excitation, P_{exc}, as measured under the objective was varied in the range of 0.001–2.0 mW. For Raman/PL measurements, the Si NCs were deposited onto the glass

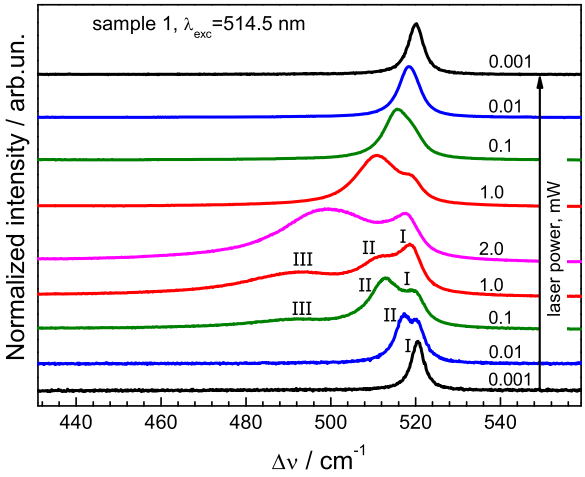

Figure 2. Normalized Raman spectra in the range of first-order optical phonons for sample 1 at varied P_{exc} of $\lambda_{exc} = 514.5$ nm. Three phonon bands distinguished in the range of the TO phonon are marked as I, II, III (see text for details). The spectra were recorded in the direction from bottom to up.

substrate. The x-ray diffraction (XRD) measurements were performed at 24, 500, and 1000 °C using the Cu K_λ line of an ARL X'tra instrument (Thermo scientific) equipped with a high-temperature chamber HTK 1200N (Anton Paar). The voltage in the tube was 45 kV, the current was 30 mA. The diffraction patterns were obtained by θ–θ-scanning (the tube and detector being rotated by the same angle).

3. Results and discussion

Figure 2 shows the representative evolution of the Raman spectra for sample 1 at varying P_{exc}. At $P_{exc} \leqslant 0.01$ mW, a single sharp peak at about 520 cm^{-1} is observed (peak I) which is characteristic for cubic Si crystals at room temperature [26]. With increasing laser power, another peak (peak II) starts to appear slightly below 520 cm^{-1}, which can be well distinguished at $P_{exc} = 0.1$ mW (figure 2).

Increasing P_{exc} by another order of magnitude leads to appearance of one more feature denoted as peak III.

Peak I shifts downwards and broadens with increasing the P_{exc} (figure 2), indicating that heating of the Si crystallites with the laser beam takes place [25]. A similar behavior can be tracked, in general, for peak II, though it cannot be resolved at $P_{exc} = 2$ mW, probably due to the overlap with peak III which first appears at about $P_{exc} = 1$ mW. At a power of 20 mW a single and much broader (FWHM ~ 30 cm^{-1}) band is observed with its maximum slightly below 500 cm^{-1} (figure 2). With the subsequent decrease of the laser power, qualitatively reversible changes in the spectrum occur, and finally it returns to the single-peak lineshape, with the position of peak I coinciding rather well with the initial spectrum at the same power of 0.01 mW but a bit larder bandwidth (figure 2). Qualitatively the same behavior as in figure 2 was also observed at $\lambda_{exc} = 488$ and 632.8 nm. At maximum powers $P_{exc} > 2$ mW the changes in the spectra were not reversible any more.

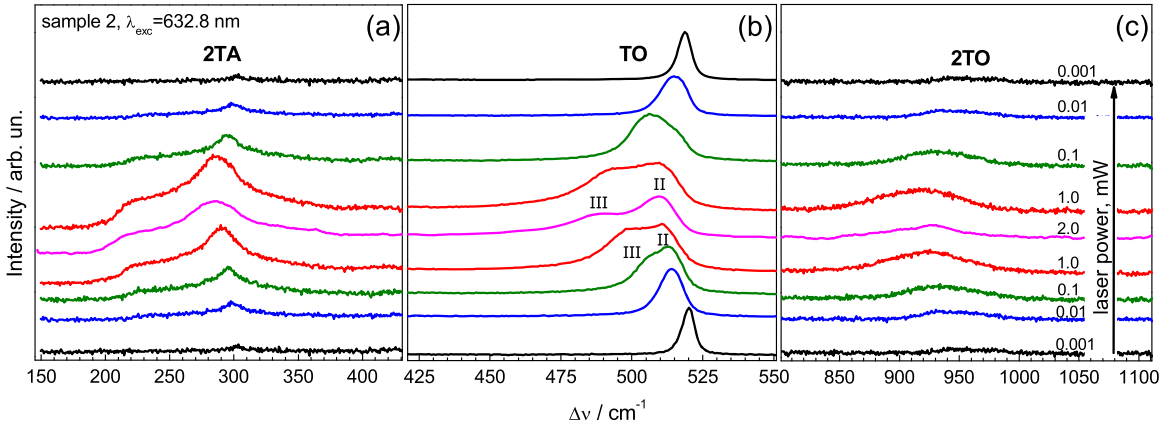

Figure 3. Raman spectra of sample 2 at varied P_{exc} of $\lambda_{exc} = 632.8$ nm, normalized to the maximum of the optical phonon peak. The ranges of 2TA (a), TO (b), and 2TO (c) phonons are scaled by a different constant for a better visibility of the spectral changes in all three regions simultaneously.

From the evolution of the Raman spectra as in figure 2 one can make a preliminary conclusion that a part of the crystallites, most probably the fraction of nanosized ones, undergoes some structural changes in response to illumination, leading to the appearance of new peaks (II and III) in the Raman spectra. Another part, presumably microcrystallites, does not contribute to this transformation and are responsible for the peak I. The behavior of the latter peak with the laser power can be related to a temperature dependence expected from heating the Si crystallites with the laser beam. We will address the temperature issue quantitatively later in the text. At this point we only note that the observed changes in the Raman spectra in figure 2 can hardly be accounted for by a size-dependent heating of the crystallites, because this would result in additional broadening of the Raman peaks rather than in additional discrete bands. Therefore, we obviously deal with a structural transformation of the Si NCs subject to intense laser illumination.

In order to check this assumption and the role of crystallite size in the effect observed in the Raman spectra, the same P_{exc}-dependent measurements were performed on sample 2 containing solely NCs (and no microcrystals). The behavior of the Raman spectra of this sample in the region of the TO mode (figure 3(b)) is similar to that of the sample 1 (figure 2), but peak I is absent (except for the initial spectrum, at 0.01 mW).

As far as sample 2 does not contain crystallites in micrometer size range, the spectral changes for this sample confirm the above made assumption about the assignment of peak I to larger crystallites which do not undergo the tentative structural transition. The difference in the spectra of samples 1 and 2 is additionally illustrated in figure 4 by representative curve fitting.

Based on the previous works on the Raman spectra of various Si polytypes [11–15, 18–22], we can assume that the new peaks in the Raman spectra indicate the transformation of cubic Si NCs into other structural polytype. The spectral position of the new Raman peaks agrees well with previous experimental and theoretical works on h-Si [16, 25, 31, 32, 34]. In particular, the reported frequencies of the Raman-active h-Si phonons are at 494–506 cm^{-1} and 516–518 cm^{-1} [11–15, 18–22, 34]. The scatter of these values can be due to different heating or stress magnitudes in different studies, or due to the overlap of phonon peaks of hexagonal and cubic phases. In some studies both Raman peaks assigned to the hexagonal structure were

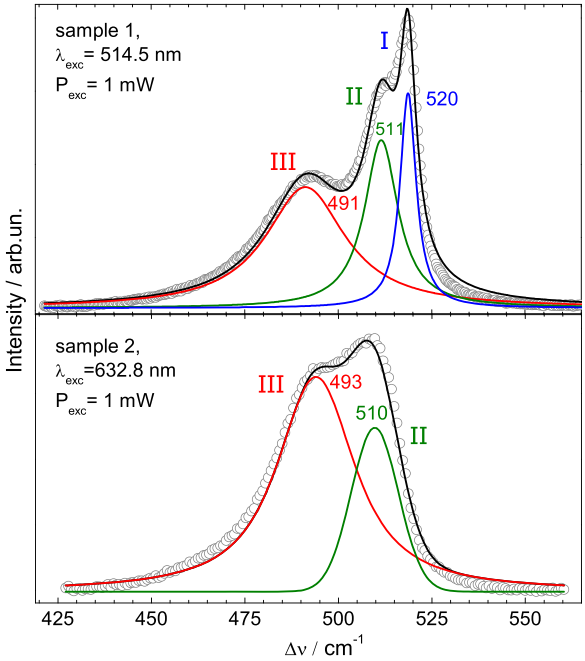

Figure 4. An example fitting of the Raman spectra of samples 1 and 2 at $P_{exc} = 1$ mW.

observed simultaneously, at 495–503 and 514–518 cm^{-1}, correspondingly [14], in agreement with theory prediction of Raman active modes at 516 (A_{1g}), 507 (E_{1g}) and 493 cm^{-1} (E_{2g}) [33].

Therefore, the evolution of the peak II in figures 2 and 3(b) we can relate with a combined effect of the laser-induced heating of the initially cubic NCs and their transformation into the hexagonal phase. The scale of the phase transformation becomes significant when the second h-Si Raman band—peak III—appears in the spectrum.

Due to its large bandwidth and spectral position the peak III may resemble the Raman feature of a-Si [32] and thus indicate some amorphization at an intermediate stage of structural transformation of Si between the cubic and hexagonal phases. However, the Raman bandwidth of a-Si is typically larger than 50 cm^{-1} [32, 35], the width of peak III is only 20–25 cm^{-1}. The proximity of the frequency positions of the a-Si band and the one of the characteristic h-Si modes can be related to the structural similarity of the short-range atomic configuration in a-Si and in h-Si structure [18, 36–38]. On the other hand, the close formation energies of the a-Si and h-Si phases [37] can be a reason for a partial amorphization of the NCs before or even after their transformation into h-Si.

Additional arguments in favor of the h-Si formation is the change of the Raman lineshape and intensity in the range of second-order scattering due to acoustical (figure 3(a)) and optical phonons (figure 3(c)). In the spectra obtained at 0.01 mW, the intensity ratio of the 2TA and 2TO bands to the TO one are equal to $I_{2TA}/I_{TO} = 0.05$ and $I_{2TO}/I_{TO} = 0.14$ in good agreement with values measured for cubic Si at room temperature [39]. For the spectra measured at 1.0–2.0 mW, i.e. where the peaks II and III are very pronounced and the strong PL appears, values of $I_{2TA}/I_{TO} = 0.2$–0.3 and $I_{2TO}/I_{TO} = 0.3$–0.35 are much higher than the corresponding ratios measured for cubic Si at temperature as high as 600 °C [23, 24]. An extrapolation of the dependences obtained in [39] to $I_{2TA}/I_{TO} = 0.2$–0.3 and $I_{2TO}/I_{TO} = 0.3$–0.35 yields temperatures around or even larger than the melting point of Si at 1300 °C. The latter fact indicates that the

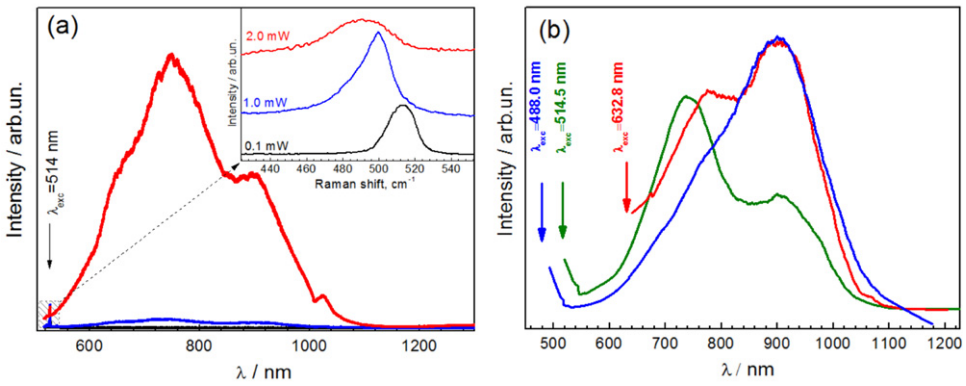

Figure 5. Photoluminescence spectra of sample 1 for $\lambda_{exc} = 514.5$ nm and varied P_{exc} (a) and for different λ_{exc} (488.0, 514.5, and 632.8 nm) at a fixed $P_{exc} = 2$ mW (b). The inset in (a) shows the corresponding Raman spectra recorded simultaneously as a part of the PL spectrum.

ratios of I_{2TA}/I_{TO} and I_{2TO}/I_{TO} are not related with the cubic Si phase, but with some other modification having larger relative intensities of second order phonon peaks compared to cubic Si. Exactly this situation was observed for h-Si in [39]—the room temperature intensity of the 2TA features of h-Si nanowires was observed to be much stronger than those of cubic Si. This is supported by the fact that the local temperatures determined in our study from the peak shifts and antistokes/stokes intensity ratios gives much more reasonable values, namely 100–200 °C for peak I and 200–400 °C for peak II at $P_{exc} = 1.0$–2.0 mW (for sample 1). Note, that the estimate based on the antistokes/stokes intensity ratio implies the applicability of the temperature dependence of the ratio derived for cubic Si earlier [25, 26, 40, 41] to h-Si. We can make the assumption of such applicability based on the room temperature value reported for h-Si in [18].

Evidence for the transformation, as well as of the particular structure resulting from it, also results from PL spectra.

Upon appearance of the additional phonon peak(s) in the Raman spectra at certain excitation power, we simultaneously observed strong PL in the red-IR spectral region (figure 5(a)). The maximum PL intensity is correlated with the most pronounced changes in the Raman spectra, that is when the downward shifts are maximum and the relative intensity of the peaks II and III is maximum. The Raman peak shown in the inset to figure 5, a recorded as a part of the PL spectrum confirms this correlation, even though the spectral resolution in the PL measurement does not allow the structure of the Raman peak in the PL spectrum to be resolved as good as in the Raman spectra of figures 2 and 3. Nevertheless, the correlation between the evolution of the PL intensity and that of the new Raman peaks is obvious.

The photoluminescent nature of the spectral features observed in figure 5(a) is confirmed by measuring the spectra with different excitation wavelengths (figure 5(b)). The spectral position of the PL bands is in good agreement with those reported for h-Si nanowires [14, 16], indicating that the additional peaks in the Raman spectra (figure 2), appearing simultaneously with the PL bands, are also related to hexagonal phase. The interplay between the PL components at ~700 and ~900 nm can be specific to the excitation wavelength, but this effect needs additional investigations, because a similar interplay was observed by changing the excitation power in [14]. Therefore, a power effect may not be excluded here as well, because

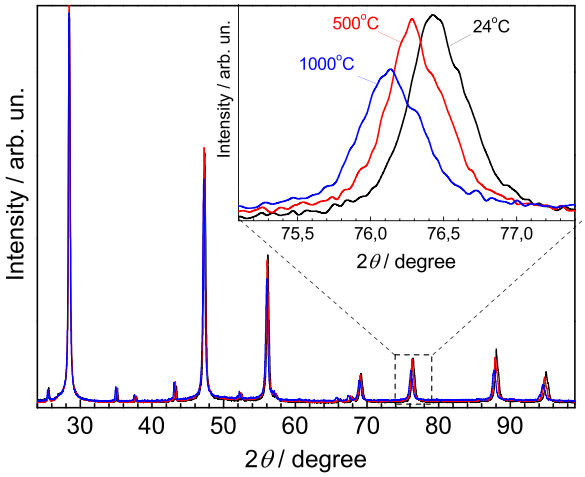

Figure 6. XRD patterns of sample 1 at different temperatures, namely 24, 500, and 1000 °C. The inset shows the region around one of the reflections in detail.

the observed transformations are highly sensitive to the degree of focusing of the laser beam. This means that the same spectral changes as in figures 2–4 can be observed by focusing–defocusing the laser spot at constant laser power of 1.0–2.0 mW.

Therefore, based on the results obtained, we can conclude that a reversible cubic-hexagonal structural transition in nanocrystalline Si takes place due to laser-induced heating. This transition is supposed to be not purely thermally induced but photo-induced, because we observed no comparable behavior in the Raman spectra at low laser power (<0.01 mW) and thermal heating up to 600 °C. As the *in situ* Raman/PL measurements during heating the sample were limited to 600 °C by the instrumental characteristics of the Linkam stage, we additionally studied Si NC samples after annealing to 1000 °C. Qualitatively the same effects were observed as for unannealed NCs. As the hexagonal phase is obviously metastable, because it transforms back to cubic one upon the reducing the laser power (figure 2), we performed an *in situ* temperature-dependent XRD study in the range of 20–1000 °C (figure 6), which revealed no structural changes in the samples even in this broader temperatures range. The temperature increase only leads to a shift of reflexes towards smaller angles and decrease of their integral intensity, as well as growth of a diffuse background (figure 6). These effects are evidence for the normal temperature-dependent behavior of the crystal lattice.

Therefore, we can conclude that the structural transformations observed in the *in situ* Raman/PL experiments are, at least partially, photo-induced. No principal difference of these transformations was noticed when excited with 488, 514, or 633 nm and comparable values of P_{exc}. This observation does not appear surprising, because a number of various structural transformations in solids are known which occur due to excitation of electronic system by absorbed electromagnetic radiation. The excitation can be either interband [42, 43], as in the case of Si NCs studied in this work, or intra-center absorption by defects or impurities, as in the case of re-orienting defects, in particular FA-centers in alkali-halide crystals [44]. Another example of well-known photo-induced transformation of crystal structures widely applied in technology is the crystallization by light-induced thermal annealing of silicon strongly disordered by high-dose ion implantation [45].

4. Conclusions

The cubic-to-hexagonal structural transformation is observed *in situ*, by increasing the power density of the laser light used for the excitation of Raman/PL spectra. The formation of the hexagonal structure is proved by the simultaneous appearance of characteristic Raman peaks near 500 cm^{-1} and intense red-IR PL. The high PL intensity indicates that the new phase formed has a direct bandgap and the spectral position of the PL band is in good agreement with that reported previously for h-Si. The phase transition is supposed to be photo-induced, as it does not occur as a consequence of solely thermal heating. The indirect-direct gap transition and concomitant PL emission observed here is reversible and is supposed to be of interest from the viewpoint of application.

Aknowledgements

The work was partially supported by the Alexander von Humboldt Foundation and Cluster of Excellence 'MERGE' (EXC 1075).

References

[1] Pavesi L and Turan R (ed) 2010 *Silicon Nanocrystals: Fundamentals Synthesis and Applications* (New York: Wiley) p 648
[2] Cheng K-Y, Anthony R, Kortshagen U R and Holmes R J 2011 High-efficiency silicon nanocrystal light-emitting devices *Nano Lett.* **11** 1952–6
[3] Kovalev D and Fujii M 2005 Silicon nanocrystals: photosensitizers for oxygen molecules *Adv. Mater.* **17** 2531–44
[4] Hessel C M, Reid D, Panthani M G, Rasch M R, Goodfellow B W, Wei J, Fujii H, Akhavan V and Korgel B A 2012 Synthesis of ligand-stabilized silicon nanocrystals with size-dependent photoluminescence spanning visible to near-infrared wavelengths *Chem. Mater.* **24** 393–401
[5] Kovalev D, Diener J, Heckler H, Polisski G, Künzner N and Koch F 2000 Optical absorption cross sections of Si nanocrystals *Phys. Rev.* B **61** 4485–7
[6] Korsunska N, Baran M, Khomenkova L, Yukhymchuk V, Goldstein Y, Savir E and Jedrzejewski J 2003 Mechanism of photoexcitation of oxide-related emission bands in Si–SiO_2 systems *Mater. Sci. Eng.* C **23** 691–6
[7] Martin J, Cichos F, Huisken F and von Borczyskowski C 2008 Electron–phonon coupling and localization of excitons in single silicon nanocrystals *Nano Lett.* **8** 656–60
[8] Hannah D C, Yang J, Podsiadlo P, Chan M K Y, Demortière A, Gosztola D J, Prakapenka V B, Schatz G C, Kortshagen U and Schaller R D 2012 On the origin of photoluminescence in silicon nanocrystals: pressure-dependent structural and optical studies *Nano Lett.* **12** 4200–5
[9] Johnson B C, Haberl B, Bradby J E, Mccallum J C and Williams J S 2011 Temperature dependence of Raman scattering from the high-pressure phases of Si induced by indentation *Phys. Rev.* B **83** 235205
[10] Lopez F J, Givan U, Connell J G and Lauhon L J 2011 Silicon nanowire polytypes: identification by raman spectroscopy generation mechanism and misfit strain in homostructures *ACS Nano* **5** 8958–66
[11] Anna B, Arbiol J, Prades J D, Cirera A and Morante J R 2007 Synthesis of silicon nanowires with wurtzite crystalline structure by using standard chemical vapor deposition *Adv. Mater.* **19** 1347–51
[12] Zhang Y, Iqbal Z, Vijayalakshmi S, Grebel H, Zhang Y, Iqbal Z, Vijayalakshmi S and Grebel H 1999 Stable hexagonal-wurtzite silicon phase by laser ablation stable hexagonal-wurtzite silicon phase by laser ablation *Appl. Phys. Lett.* **75** 2758–60

[13] Cao L, Laim L, Ni C, Nabet B and Spanier J E 2005 Diamond-hexagonal semiconductor nanocones with controllable apex angle *J. Am. Chem. Soc.* **127** 13782–3
[14] Bandet J, Despax B and Caumont M 2002 Vibrational and electronic properties of stabilized wurtzite-like silicon *J. Phys. D: Appl. Phys.* **35** 234–9
[15] Kailer A, Gogotsi Y G, Nickel K G, Kailer A, Gogotsi Y G and Nickel K G 1997 Phase transformations of silicon caused by contact loading *J. Appl. Phys.* **81** 3057–63
[16] Kim T-Y, Huh C, Park N-M, Choi C and Suemitsu M 2012 *In situ*-grown hexagonal silicon nanocrystals in silicon carbide-based films *Nanoscale Res. Lett.* **7** 634
[17] Fabbri F, Rotunno E, Lazzarini L, Fukata N and Salviati G 2014 Visible and infra-red light emission in boron-doped wurtzite silicon nanowires *Sci. Rep.* **4** 3603
[18] Wu K, Yan X Q, Chen M W, Wu K, Yan X Q and Chen M W 2007 *In situ* Raman characterization of reversible phase transition in stress-induced amorphous silicon *Appl. Phys. Lett.* **91** 101903
[19] Nikolenko A, Strelchuk V, Klimovskaya A, Lytvyn P, Valakh M, Pedchenko Y, Voroschenko A and Hourlier D 2011 Scanning confocal Raman spectroscopy of silicon phase distribution in individual Si nanowires *Phys. Status Solidi* C **8** 1012–6
[20] Prades J D, Arbiol J, Cirera A, Morante J R and Morral A F 2007 Concerning the 506 cm^{-1} band in the Raman spectrum of silicon nanowires *Appl. Phys. Lett.* **91** 123107
[21] Lopez F J, Hemesath E R and Lauhon L J 2009 Ordered stacking fault arrays in silicon nanowires *Nano Lett.* **9** 2774–9
[22] Peng Z, Hu H, Iqbal M, Utama B, Wong L M, Ghosh K, Chen R, Wang S, Shen Z and Xiong Q 2010 Heteroepitaxial decoration of Ag nanoparticles on Si nanowires: a case study on raman scattering and mapping *Nano Lett.* **10** 3940–7
[23] Tarun A, Hayazawa N, Ishitobi H, Kawata S, Reiche M and Moutanabbir O 2011 Mapping the 'forbidden' transverse-optical phonon in single strained silicon (100) nanowire *Nano Lett.* **11** 4780–8
[24] Scheel H, Khachadorian S, Cantoro M, Colli A, Ferrari A C and Thomsen C 2008 Silicon nanowire optical Raman line shapes at cryogenic and elevated temperatures *Phys. Status Solidi* B **245** 2090–3
[25] Lo H W and Compaan A 1980 A Raman measurements of temperature during cw laser heating of silicon *J. Appl. Phys.* **51** 1565–8
[26] Hart T R and Lax B 1970 Temperature dependence of Raman scattering in silicon *Phys. Rev.* B **1** 638–42
[27] Faraci G, Gibilisco S and Pennisi A R 2009 Superheating of silicon nanocrystals observed by Raman spectroscopy *Phys. Lett.* A **373** 3779–82
[28] Faraci G, Gibilisco S and Pennisi A R 2009 Quantum confinement and thermal effects on the Raman spectra of Si nanocrystals *Phys. Rev.* B **80** 193410
[29] Gibilisco S, Faraci G, Pennisi A R and Irrera A 2010 Laser induced heating of Si nanocrystals *J. Non-Cryst. Solids* **356** 1948–50
[30] Faraci G, Gibilisco S, Russo P, Pennisi A R, Compagnini G, Battiato S, Puglisi R and La Rosa S 2005 Si/SiO_2 core–shell clusters probed by Raman spectroscopy *Eur. Phys. J.* B **46** 457–61
[31] Kobliska R J and Solin S A 1973 Raman spectrum of wurtzite silicon *Phys. Rev.* B **8** 3799–802
[32] Azhniuk Y M, Schäfer P, Gomonnai A V, Misiuk A, Prujszczyk M and Zahn D R T 2010 MicroRaman studies of implantation-induced amorphization of Si and subsequent regrowth under high-pressure and high-temperature treatment *Phys. Status Solidi* A **207** 2432–6
[33] Wu B R 2000 First-principles study on the high-pressure behavior of the zone-center modes of lonsdaleite silicon *Phys. Rev.* B **61** 5–8
[34] Gogotsi Y, Baek C and Kirscht F 1999 Raman microspectroscopy study of processing-induced phase transformations and residual stress in silicon *Semicond. Sci. Technol.* **14** 936–44
[35] Iqbal Z and Vepřek S 1982 Raman scattering from hydrogenated microcrystalline and amorphous silicon *J. Phys. C: Solid State Phys.* **15** 377–92
[36] Rudee M L and Howie A 1972 The structure of amorphous Si and Ge *Phil. Mag.* **25** 1001–7

[37] Domnich D, Ge V and Gogotsi Y 2004 Thermal stability of metastable silicon phases produced by nanoindentation *J. Appl. Phys.* **95** 2725–30
[38] Wu Y Q, Yang X Y and Xu Y B 1999 Cross-sectional electron microscopy observation on the amorphized indentation region in [001] single-crystal silicon *Acta Mater.* **47** 2431–6
[39] Khachadorian S, Scheel H, Colli A, Vierck A and Thomsen C 2010 Temperature dependence of first- and second-order Raman scattering in silicon nanowires *Phys. Status Solidi* B **247** 3084–8
[40] Abel M R, Wright T L, King W P and Graham S 2007 Thermal metrology of silicon microstructures using Raman spectroscopy *IEEE Trans. Compon. Packag. Technol.* **30** 200–8
[41] Tsu R and Gonzalez-Hernandez J 1982 Temperature dependence of silicon Raman lines *Appl. Phys. Lett.* **41** 1016–8
[42] Artamonov V V, Valakh M Y, Denisov A V, Mordkovich V N and Nechiporuk B D 1992 *Sov. Phys. Semicond.* **26** 1169
[43] Valakh M Y, Dzhagan V M, Babichuk I S, Fontane X, Perez-Rodriguez A and Schorr S 2013 Optically induced structural transformation in disordered kesterite Cu_2ZnSnS_4 *JETP Lett.* **98** 255–8
[44] Brodin A M, Boiko S A, Valakh M Y and Tarasov G G 1988 Effect of optical feedback on self-induced change of light polarization in cubic crystals with directions instable for polarization *Phys. Status Solidi* B **150** 557–60
[45] Nylandsted L A and Borisenko V E 1984 Behavior of implanted arsenic in silicon single crystals subjected to transient heating with incoherent light *Appl. Phys.* A **33** 51–8